

# Direct Evaluation of the Helium Abundances in Omega Centauri

A. K. Dupree and E. H. Avrett

Harvard-Smithsonian Center for Astrophysics, Cambridge, MA 02138, USA

dupree@cfa.harvard.edu; eavrett@cfa.harvard.edu

Received \_\_\_\_\_; accepted \_\_\_\_\_

ApJ Letters, in press

arXiv:1307.5860v1 [astro-ph.SR] 22 Jul 2013

## ABSTRACT

A direct measure of the helium abundances from the near-infrared transition of He I at  $1.08\mu\text{m}$  is obtained for two nearly identical red giant stars in the globular cluster Omega Centauri. One star exhibits the He I line; the line is weak or absent in the other star. Detailed non-LTE semi-empirical models including expansion in spherical geometry are developed to match the chromospheric  $\text{H}\alpha$ ,  $\text{H}\beta$ , and Ca II K lines, in order to predict the helium profile and derive a helium abundance. The red giant spectra suggest a helium abundance of  $Y \leq 0.22$  (LEID 54064) and  $Y = 0.39 - 0.44$  (LEID 54084) corresponding to a difference in the abundance  $\Delta Y \geq 0.17$ . Helium is enhanced in the giant star (LEID 54084) that also contains enhanced aluminum and magnesium. This direct evaluation of the helium abundances gives observational support to the theoretical conjecture that multiple populations harbor enhanced helium in addition to light elements that are products of high-temperature hydrogen burning. We demonstrate that the  $1.08\mu\text{m}$  He I line can yield a helium abundance in cool stars when constraints on the semi-empirical chromospheric model are provided by other spectroscopic features.

*Subject headings:* stars: individual (LEID 54064, LEID 54084 ) - stars: abundances - stars: atmospheres - globular clusters: individual (Omega Centauri)

## 1. Introduction

Our current understanding of stellar populations in globular clusters has dramatically changed with the discoveries of multiple stellar generations in a single globular cluster. While variations in color and a spread in the  $[\text{Fe}/\text{H}]$  values of red giants in massive clusters have been long recognized (Woolley 1966, Geyer 1967) along with variations of light elements (Martell 2011), the firm identification of multiple populations on the main sequence in Omega Centauri (Anderson 1997; Bedin et al. 2004; Bellini et al. 2010), and subsequently several other clusters (cf. Gratton et al. 2012), was surprising and continues to present theoretical challenges. Norris (2004) suggested, based on isochrone calculations, that dwarf stars on the ‘blue’ main sequence in Omega Cen would be enhanced in helium by  $\Delta Y \sim 0.10\text{--}0.15$ . The lowered hydrogen opacity causes stars of the same mass to appear hotter and more luminous (Valcarce et al. 2012). Subsequently, the assessment of metals in dwarfs on the bifurcated main sequence in Omega Cen, showed that the hotter objects (the ‘blue’ dwarfs) were less metal-poor than the ‘red’ dwarf stars (Piotto et al. 2005). Stellar models suggest that increased metals also signal the presence of enhanced helium in the ‘blue’ main sequence. The source (or sources) of such an enhancement remains elusive. One attractive explanation appears to be a second stellar generation formed from the material lost by the first generation of intermediate mass stars during their asymptotic giant phases (D’Ercole et al. 2010; Johnson & Pilachowski 2010; Renzini 2013), although other possibilities such as fast-rotating massive stars (Charbonnel et al. 2013) or massive binary-star mass overflow (de Mink et al. 2009) may well contribute (cf. Gratton et al. 2012). The formation of cluster populations with several generations of star formation also impacts an understanding of the halo of the Milky Way, satellites of our Galaxy, and the star formation and assembly history of other galaxies (cf. Gratton et al. 2012; Brodie & Strader 2006).

It is obviously of great interest if a helium enhancement could be verified in globular cluster stars in our Galaxy. A direct measure of the helium abundance from a spectrum would provide confirmation of Norris’ conjecture. Such a measurement is challenging because useful lines of helium are generally absent in the optical spectra of cool stars. Moreover, in hotter stars, such as blue horizontal branch objects, sedimentation caused by diffusion and element stratification occur. Helium abundances from the spectroscopy of hot horizontal branch stars in Omega Cen demonstrate the effects of surface diffusion, or mixing during late helium core flashes (DaCosta et al. 1986; Moehler et al. 2011; Moni Bidin et al. 2012) and derived abundance values vary widely from  $Y \leq 0.02$  to  $Y=0.9$ .

In cool stars, a transition in He I occurs in the near-infrared at  $1.08\mu\text{m}$  and has been identified in many metal-poor field stars, where, in addition to abundances, it can indicate atmospheric dynamics because the lower level of the transition is metastable (Dupree et al. 1992, 2009; Smith et al. 2012). In Omega Centauri, a closely matched group of first-ascent red giant stars displays strong and weak helium absorption that correlates (Dupree et al. 2011) with increased  $[\text{Al}/\text{Fe}]$  and  $[\text{Na}/\text{Fe}]$  abundance, more than with  $[\text{Fe}/\text{H}]$ . This result gave direct observational support to the idea that products of high-temperature hydrogen burning in a previous stellar generation had, in fact, occurred. A quantitative measure of the helium abundance in these objects is the goal of this Letter.

Pasquini et al. (2011) calculated profiles of the He I  $1.08\mu\text{m}$  line in an approximate way based on a stationary plane-parallel model applied to two very cool luminous stars in NGC 2808. They showed that a change in the chromospheric structure itself can strengthen or weaken helium absorption. In fact, chromospheric line profiles are highly sensitive to the structure and dynamics of the atmospheric model. In this paper, we have selected similar stars and first constrained the atmospheric structure and dynamics using other chromospheric lines. A model for the radiative transfer must be used that is appropriate to

the stars. Following that, the abundance of helium can be inferred from line synthesis using the semi-empirical atmospheric model that is anchored by other chromospheric lines.

Here we focus on two ‘identical’ red giants in Omega Centauri, LEID 54064 and LEID 54084 (van Leeuwen et al. 2000). They are located  $\sim 5.7$  arc min to the SW from the cluster center, and are separated by 1.6 arcminutes on the sky. These giants have very similar temperatures, luminosities, and values of  $[\text{Fe}/\text{H}]$  (Table 1). However they differ remarkably in  $[\text{Na}/\text{Fe}]$  and  $[\text{Al}/\text{Fe}]$  abundances and the strength of the helium line (Dupree et al. 2011). The star LEID 54084 exhibits enhanced light elements as compared to LEID 54064.

## 2. Modeling Chromospheric Lines

The PANDORA code (Avrett & Loeser 2003, 2008) is used to develop the semi-empirical, spherical model of the chromosphere where the temperature distribution, the turbulent velocities, and the expansion velocities are adjusted to obtain optimum agreement between calculated profiles and observations of chromospheric lines ( $\text{H}\alpha$ ,  $\text{H}\beta$ , and Ca II-K). The initial model consists of a static LTE photosphere corresponding to a effective temperature of 4740K (Kurucz 2011), gravity  $\log g = 1.75$ , a stellar radius of  $20R_{\odot}$ , and  $[\text{Fe}/\text{H}] = -1.72$  with the  $\alpha$ -abundances enhanced by +0.44 dex. Chromospheric line emission is essentially unaffected by the photospheric model. A chromospheric structure similar to other metal-poor models (Mészáros et al. 2009) was added to begin the iterations, and expansion started in the low chromosphere. Our calculations assume multi-level atoms (H I: 15 levels, Ca II: 5 levels, He I: 13 levels), and the iterations explicitly consider the velocity field in the evaluation of the line source functions and as a contribution to the pressure in the hydrostatic equilibrium equations. The total model is iterated with full and complete non-LTE calculations in order to match the chromospheric line profiles. The Ca II-K line profile is computed with partial frequency redistribution; complete

frequency redistribution is used for the hydrogen and helium lines. These flux profiles are calculated with an integration over the apparent spherical stellar disk including the extended chromosphere.

The profiles of the optical lines,  $H\alpha$ ,  $H\beta$ , and Ca II-K were taken from spectra obtained with the MIKE double echelle spectrograph (Bernstein et al. 2003) mounted on the Magellan/CLAY telescope at Las Campanas Observatory. These spectra were used previously to derive elemental abundances (Dupree et al. 2011). The spectra and the calculated stellar profiles for  $H\alpha$ ,  $H\beta$ , and Ca II-K are shown in Fig. 1. The observed profiles are effectively identical between the two giants, signaling that the activity levels of the stars are similar. The spectra are well matched by the calculated profiles. Note the asymmetry in the  $H\alpha$  line core; the core is formed higher in the atmosphere than the rest of the profile and is sensitive to the outflow. However the line itself is narrow, and demands a relatively low turbulent velocity, which increases with height in the chromosphere. The final model (Fig. 2) has a temperature that extends to  $10^5\text{K}$  (although such high temperatures do not affect the profiles evaluated here), and an outflow velocity that reaches  $100\text{ km s}^{-1}$ , which yields a mass outflow rate of  $\sim 3 \times 10^{-9} M_{\odot} \text{ yr}^{-1}$ . This rate follows straightforwardly from the atmospheric model (Fig. 2) and is proportional to  $Nvr^2$  in the chromosphere, where  $r$  is the radial distance at which the wind has a velocity  $v$ , and  $N$  is the hydrogen density. This value exceeds by a factor of 1.3–1.5 the rate estimated from an extension of the Mészáros et al. (2009) fit to  $H\alpha$  profiles of cooler stars shown in their Fig. 10. For more luminous stars in the more metal-rich NGC 2808, Mauas et al. (2006) find values of  $0.7 - 3.8 \times 10^{-9} M_{\odot} \text{ yr}^{-1}$  from the  $H\alpha$  line. Field metal-poor giants, comparable in  $M_{bol}$  to our targets possess a mass loss rate spanning  $1.3 \times 10^{-9} - 10^{-8} M_{\odot} \text{ yr}^{-1}$  (Dupree et al. 2009). While mass loss rates have been measured (Mészáros et al. 2009) to vary with time by factors of 1.5 to 6 in metal-poor red giants with luminosity  $\log L/L_{\odot} \sim 3.0$ , the values inferred from semi-empirical model fits are less by an order of magnitude than the Reimers

(1977), Origlia et al. (2007), or the Schröder & Cuntz (2005) approximations.

This temperature and velocity model (Fig. 2) is used to evaluate the profile of the He I  $1.08\mu\text{m}$  line. The near-ir He I lines measured with PHOENIX on Gemini-S were reported earlier (Dupree et al. 2011). The populations, ionization fraction, and continuum emission, are evaluated in separate models for each value of the helium abundance, and the profile is calculated assuming spherical geometry in an expanding atmosphere. The contribution of the extended chromosphere can be noted in the weak emission present on the long wavelength side of the line. The helium absorption extends substantially towards shorter wavelengths due to scattering in the expanding atmosphere and is enhanced by the metastable nature of the lower level of the transition. The helium lines are essentially P Cygni profiles since the red giants have extended atmospheres. The population of the lower level of the  $1.08\mu\text{m}$  transition peaks at  $T=18,000\text{K}$ , but lies within a factor of two of its maximum value between  $14,000$  and  $25,000\text{K}$ ; the outflow velocity doubles over this temperature span.

Various values of the helium abundance, from  $Y=0.15$  to  $Y=0.50$  [ $\log(n_{\text{He}}/n_{\text{H}})$  ranging from  $10.65$  to  $11.4$ ], were assumed and 9 models calculated. The abundance selected minimizes the residuals between the observed and calculated profiles. The star LEID 54084 clearly exhibits a broad helium line which could extend to shorter wavelengths beyond the Si I absorption at  $1.027\mu\text{m}$  but is compromised by the presence of the water vapor blend with Si I. A value of  $Y=0.39$  to  $Y=0.44$  well represents the depth of the observed profile representing the minimum range in the residuals. Helium is not clearly detected in LEID 54064. The calculated profiles for  $Y\leq 0.22$  give a minimum in the residuals, and we adopt this value as an upper limit to  $Y$ . Inspection of the helium profiles shows that a value of  $Y=0.25$  overpredicts the strength of the line in LEID 54064, and the residuals of the fit are larger than for  $Y=0.22$ . These simulations suggest that the helium abundance difference is

$\Delta Y \geq 0.17$  between the two stars.

### 3. Discussion and Conclusions

This spectroscopic value of helium from LEID 54084, namely  $Y=0.39-0.44$  can be compared to values obtained from models of stellar structure and evolution. In Omega Cen, Norris (2004) estimated the presence of helium from isochrones matching the lower main sequence with values of  $Y$  ranging from 0.23 to 0.38. Piotto et al. (2005) noted the blue main sequence could only be matched with stellar models with helium abundance ranging from  $0.35 < Y < 0.45$  and concluded that  $Y=0.38$  best fit the ridgelines in the color-magnitude diagram of Omega Cen. HST photometry of an outer field in the cluster (King et al. 2012), reveals a helium abundance for the blue main sequence of  $Y=0.39\pm 0.02$ . Recent Yonsei-Yale isochrones for several subpopulations in Omega Cen (Joo & Lee 2013) suggest a range in  $Y$  from 0.38 to 0.41. Thus the spectroscopic value of helium for LEID 54084, a star with enhanced light element abundances is in harmony with the abundance inferred from stellar structure models. In a more metal rich cluster, NGC 2808, the approximate model of Pasquini et al (2011) suggested one star may have a similar value of  $Y=0.39$  to 0.5.

The  $Y$  value for LEID 54064 where the helium line is weak (or not detected) has an upper limit ( $Y \leq 0.22$ ) that is slightly less than the cosmic value ( $Y=0.24$ ). These abundances suggest the helium enhancement,  $\Delta Y$ , is  $\geq 0.17$ . King et al. (2012) concluded from plausible fits to the color magnitude diagram of Omega Cen that  $\Delta Y \sim 0.15$  where a value for the primeval abundance of helium ( $Y=0.24$ ) was chosen for the red main sequence. Piotto et al. (2005) required  $\Delta Y=0.14$  to explain the differences in metal abundances found for the blue and red main sequences. It is interesting to note that the Sun requires a helium abundance of  $Y=0.27-0.28$  to match the solar luminosity, but due to diffusion and settling,

the helium abundance in the envelope is less,  $Y=0.24-0.25$  (Christensen-Dalsgaard 2002; Guzik & Cox 1993), and  $Y=0.16$  (corresponding to  $n_{He}/n_H=0.05$ ) in the steady-state solar wind (Kasper et al. 2007). It may be that spectroscopy will yield different values for the helium abundance from those inferred from stellar isochrone models, although currently we do not know if the characteristics of the solar abundance pattern occur in these metal-poor giant stars.

The optical and near-infrared spectra used here were acquired about 3 months apart, and a variation in the line profiles might occur. However, these giants have  $\log L/L_\odot \sim 2.2$ , and  $M_V \sim -0.45$  and lie on the red giant branch below the stars that exhibit  $H\alpha$  wing emission. It is this emission which can vary in strength in first-ascent red giants (Mészáros et al. 2008; Cacciari et al. 2004). The remarkable similarity of  $H\alpha$ ,  $H\beta$ , and Ca II-K profiles between the two giants suggests that activity does not cause significant changes.

Another consideration might be the presence of X-rays or EUV emission from a high temperature plasma. Because neutral helium can be photoionized and then recombine preferentially into the lower level of the  $1.08\mu\text{m}$  line, this process would enhance the strength of the observed helium line. Red giants need substantial magnetic confinement of material to produce hot plasma; magnetic signatures in the spectra of similar stars have not been detected, and the coronae appear absent (Rosner et al. 1995). The slightly metal-poor K giant,  $\alpha$  Boo, has a ‘tentative detection’ (Ayres et al. 2003) of X-rays but, if indeed present, they are a factor of  $10^4$  weaker in  $L_X/L_{bol}$  than the average solar value and would seem to have little effect on the profile.<sup>1</sup> In  $\alpha$  Boo, the equivalent width of the  $1.083\mu\text{m}$  line varies in absorption strength which could be caused by wind variation as well

---

<sup>1</sup>*CHANDRA* images of Omega Cen (Cool et al. 2013) do not reach faint sources ( $L_X \lesssim 10^{29} \text{ erg s}^{-1}$ ). The identified optical counterparts of the X-ray sources are binaries, and not the single red giants that are targeted here.

as chromospheric excitation conditions (O’Brien & Lambert 1986). Single metal-poor red giants in the field also display a very weak  $1.08\mu\text{m}$  absorption line, and though these stars are optically brighter, they have not been detected in X-rays. Population I giants, which generally exhibit X-rays, have stronger helium absorption as compared to their metal-poor field counterparts (cf. Dupree et al. 2009). This suggests the line is not influenced by X-rays in the metal-poor stars. The Ca II-K lines are very similar in the two giants (Fig. 1) indicating that these stars have similar chromospheres such that X-rays would not be present in only one star causing the strengthening of the helium absorption. Thus it does not appear likely that X-rays contribute to the line formation for the targets considered here. Several epochs of measurement would clearly be useful to determine if variation occurs in the helium lines.

Pasquini et al. (2011) carried out a similar calculation for two stars in the globular cluster NGC 2808. The 2 luminous stars ( $\log L/L_{\odot} \sim 3.2$ ) selected by Pasquini et al. (2011) have different levels of activity as indicated by the Ca K line which underscores the ubiquitous variability of such luminous giants. These differences demand different semi-empirical models for the two stars yet only one model was used; in addition the observations of the optical and infrared spectra were separated by some weeks which brings uncertainty when modeling such luminous active objects. Computation of the line profiles in Pasquini et al. invokes models that do not adequately represent the stars nor the conditions in their atmospheres. The use of a plane-parallel approximation is questionable when modeling a star of radius  $\sim 84 R_{\odot}$ . The computation assumed a static atmosphere, and the authors simply shifted the calculated line in wavelength to match observations. However, the spectra show that the chromosphere, as measured by  $\text{H}\alpha$ , Ca K, and the helium line, exhibits signatures of outflow. We have taken our model and calculated the helium profile under the same assumptions adopted by Pasquini et al. (2011) (plane parallel and static) for comparison to a model with the appropriate assumptions for these stars, namely spherical

geometry and expanding. The results of this calculation show substantial differences. Not only does the spherical model exhibit emission, but the absorption is larger than the static model due to the expanding atmosphere. A larger star, with extended chromosphere and/or wind, might be expected to exhibit more substantial changes. For the same value of the helium abundance, the equivalent width of the absorption in the expanding spherical model is larger by 5 to 19% than the static plane-parallel model depending on the value of  $Y$ . (Here we assumed  $Y=0.28$  and  $Y=0.44$ .) Thus, interpreting the observed profile formed in an expanding large giant star, by 'matching it' to a static, plane parallel profile, as did Pasquini et al. (2011), will lead to an overestimate of the abundance of helium. Pasquini et al. (2011) do not compare the computed profiles of Ca K and  $H\alpha$ , to the stellar spectra so the adequacy of the models is unknown. Consideration of all of these facts indicates that the determination of the helium abundance in Pasquini et al. (2011) must be approached with caution.

The targets selected in this paper are of much lower luminosity where variability is absent or greatly minimized. Moreover, the 2 stars are effectively identical in temperature, luminosity, iron abundance, activity, and in chromospheric features - with the exception of helium and enhanced Al and Mg. The treatment of the radiative transfer is state of the art with a spherical atmosphere, assuming an outflow, where the outflow is incorporated into the source function for the lines.

The abundance of helium and its variation between these two giant stars in Omega Cen gives quantitative observational confirmation of a helium enhancement to accompany the enhanced light metals. The near-ir line of He I can provide a probe of the helium abundance in cool stars when additional chromospheric profiles are available to constrain the atmospheric structure and dynamics and appropriate radiative transfer calculations are employed.

We are grateful to Bob Kurucz who calculated specific photospheric models to initiate the calculations.

*Facilities:* Gemini:South (PHOENIX), Magellan:Clay (MIKE)

## REFERENCES

- Alonso, A., Arribas, S., & Martinez-Roger, C. 1999, *A&AS*, 140, 261
- Anderson, J. 1997, PhD thesis, Univ. California, Berkeley
- Avrett, E. H., & Loeser, R. 2003, in *IAU Symp. 210, Modeling of Stellar Atmospheres*, ed. W. Weise & N. Piskunov (Dordrecht: Kluwer), A-21
- Avrett, E. H., & Loeser, R. 2008, *ApJS*, 175, 229
- Ayres, T., Brown, A., & Harper, G. M. 2003, *ApJ*, 598, 610
- Bedin, L. R., Piotto, G., Anderson, J., et al. 2004, *ApJ*, 605, L125
- Bellini, A., Bedin, L. R., Piotto, G., et al. 2010, *AJ*, 140, 631
- Bernstein, R. A., Sackett, S. A., Gunnels, S. M., Mochnacki, S., & Athey, A. E. 2003, *Proc. SPIE*, 4841, 1694
- Brodie, J. P., & Strader, J. 2006, *ARA&A*, 44, 193
- Cacciari, C., Bragaglia, A., Rossetti, E. et al. 2004, *A&A*, 413, 343
- Charbonnel, C., Krause, M., Decressin, T., Prantzos, N., & Meynet, G. 2013, arXiv 1301.5016
- Christensen-Dalsgaard, J. 2002, *Rev. Mod. Phys.*, 74, 1073
- Cool, A. M., Haggard, D., Arias, T., et al. 2013, *ApJ*, 763, 126
- DaCosta, G. S., Norris, J., & Villumsen, J. V. 1986, *ApJ*, 308, 743
- deMink, S. E., Pols, O. R., Langer, N., & Izzard, R. G. 2009, *A&A*, 507, L1
- D’Ercole, A., D’Antona, F., Ventura, P., Vesperini, E., & McMillan, S. L. W. 2010, *MNRAS*, 407, 854
- Dupree, A. K., Sasselov, D. D. & Lester, J. B. 1992, *ApJ*, 387, L85

- Dupree, A. K., Smith, G. H., & Strader, J. 2009, *AJ*, 138, 1485
- Dupree, A. K., Strader, J., & Smith, G. H. 2011, *ApJ*, 728, 155
- Geyer, E. H. 1967, *ZAp*, 66, 16
- Gratton, R. G., Carretta, E., & Bragaglia, A. 2012, *A&A Rev.*, 20, 50
- Guzik, J. A., & Cox, A. N. 1993, *ApJ*, 411, 394
- Johnson, C. J., & Pilachowski, C. A. 2010, *ApJ*, 722, 1373
- Joo, S. J., & Lee, Y. W. 2013, *ApJ*, 762, 36
- Kasper, J.C., Stevens, M. L., Lazarus, A. J., Steinberg, J. T., & Ogilvie, K. W. 2007, *ApJ*, 660, 901
- King, I. R., Bedin, L. R., Cassisi, S., et al. 2012, *AJ*, 144, 5
- Kurucz, R. L. 2011, *Can. J. Phys.*, 89, 417
- Martell, S. L. 2011, *AN*, 332, 467
- Mauas, P. J. D., Cacciari, C., & Pasquini, L. 2006, *A&A*, 454, 609
- Mészáros, Sz., Dupree, A. K., & Szentgyorgyi, A. 2008, *AJ*, 135, 1117
- Mészáros, Sz., Avrett, E. H., & Dupree, A. K. 2009, *AJ*, 138, 615
- Moehler, S., Dreizler, S., Lanz, T., et al. 2011, *A&A*, 526, A136
- Moni Bidin, C., Villanova, S., Piotto, G., et al. 2012, *A&A*, 547, A109,
- Norris, J. E. 2004, *ApJ*, 612, L25
- O’Brien, G. T., & Lambert, D. L. 1986, *ApJS*, 62, 899
- Origlia, L, Rood, R. T., Fabbri, S. et al. 2007, *ApJ*, 667, L85
- Pasquini, L., Mauas, P., Käuffl, J. U., & Cacciari, C. 2011, *A&A*, 531, A35
- Piotto, G., Villanova, S., Bedin, L. R., et al. 2005, *ApJ*, 621, 777

- Reimers, D. 1975, Mem. Soc. R. Sci Liège, 8, 369
- Renzini, A. 2013, Mem. S. A. It., in press (arXiv:1302.0329)
- Rosner, R., Musielak, Z. E., Cattaneo, F., Moore, R. L., & Suess, S. T. 1995, ApJ, 442, L25
- Schröder, K.-P., & Cuntz, M. 2005, ApJ, 630, L73
- Skrutskie, M. F., Cutrie, R. M., Stiening, R. et al. 2006, AJ, 131, 1163
- Smith, G. H., Dupree, A. K., & Strader, J. 2012, PASP, 124, 1252
- Valcarce, A. A. R., Catelan, M. & Sweigart, A. V. 2012, A&A, 547, A5
- van Leeuwen, F., Le Poole, R. S., Reijns, R. A., Freeman, K. C., & de Zeeuw, P. T. 2000,  
A&A, 360, 472
- Woolley, r. v. d. R. 1966, R. Obs. Ann., 2,1

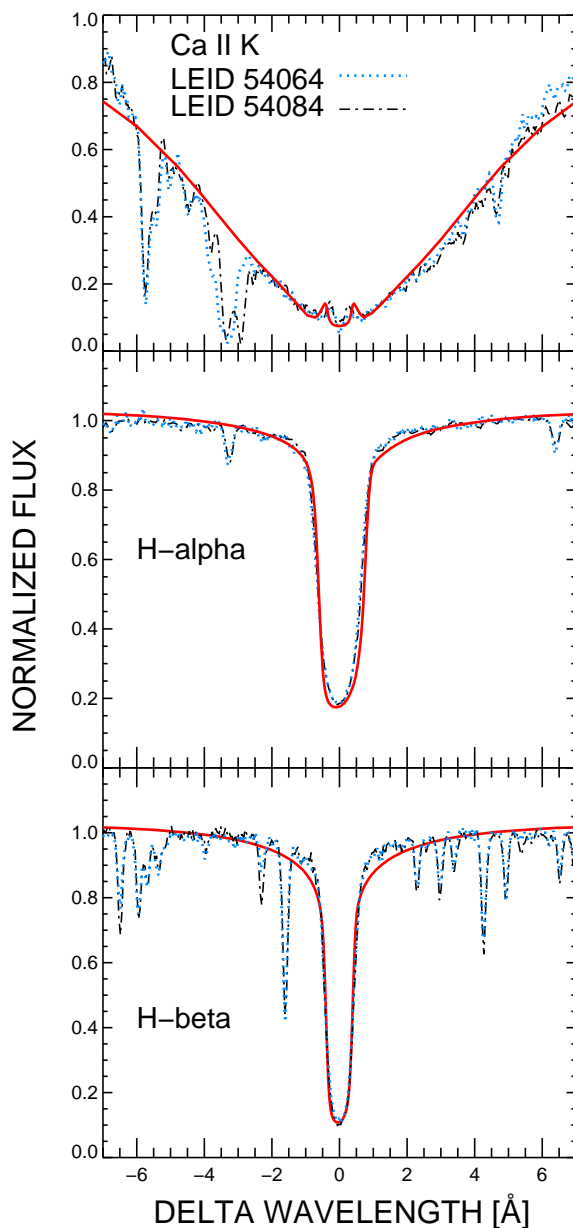


Fig. 1.—  $H\alpha$  ,  $H\beta$ , and Ca II K-line region shown for the two giant stars with the model fit overlaid (*indicated by a solid line which is colored red in the electronic edition*). The spectra of the two stars are virtually identical. The Ca II spectrum displays an interstellar absorption feature blended with the Fe I line at  $-3\text{\AA}$  from the line core in the LEID 54064 spectrum, but distinct from the Fe I feature in the LEID 54084 spectrum. Weak emission may be present on the long-wavelength wing of the  $H\alpha$  line and on both wings of the  $H\beta$  line. The success of the model can be seen from the agreement between observed and calculated chromospheric profiles. A color version of this figure is in the electronic edition.

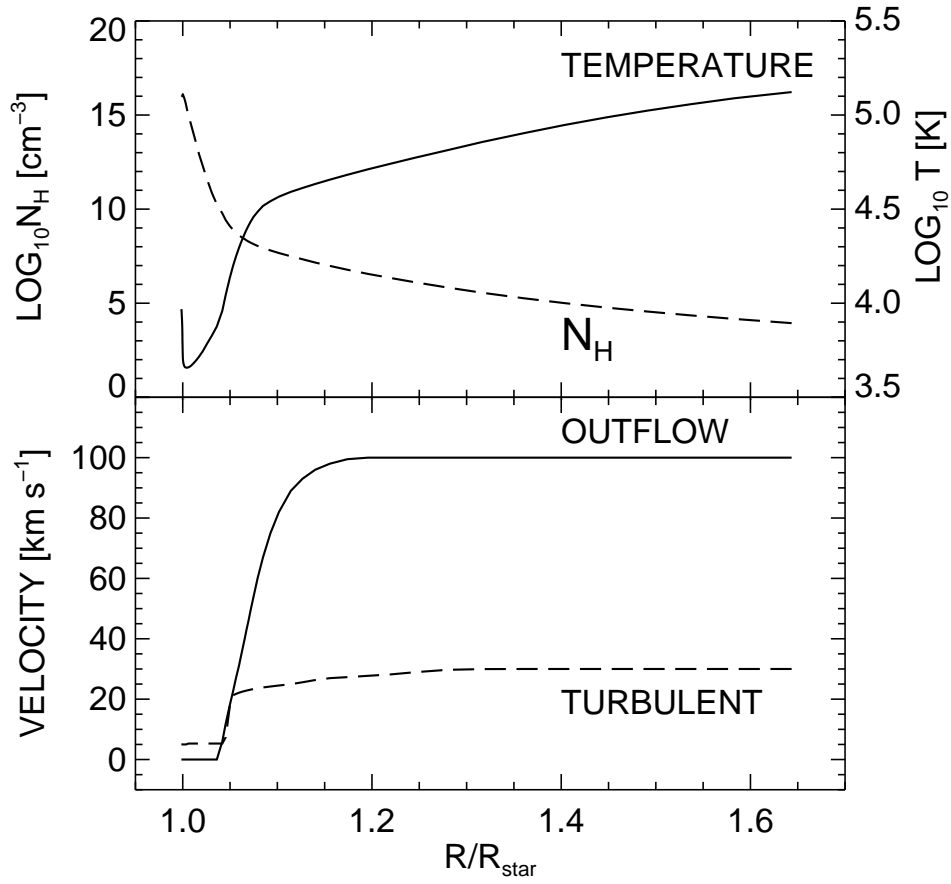


Fig. 2.— Final model. The top panel displays the total hydrogen density (*left axis*) and the temperature (*right axis*). The lower panel shows the turbulent and outflow velocities needed to match the observed profiles.

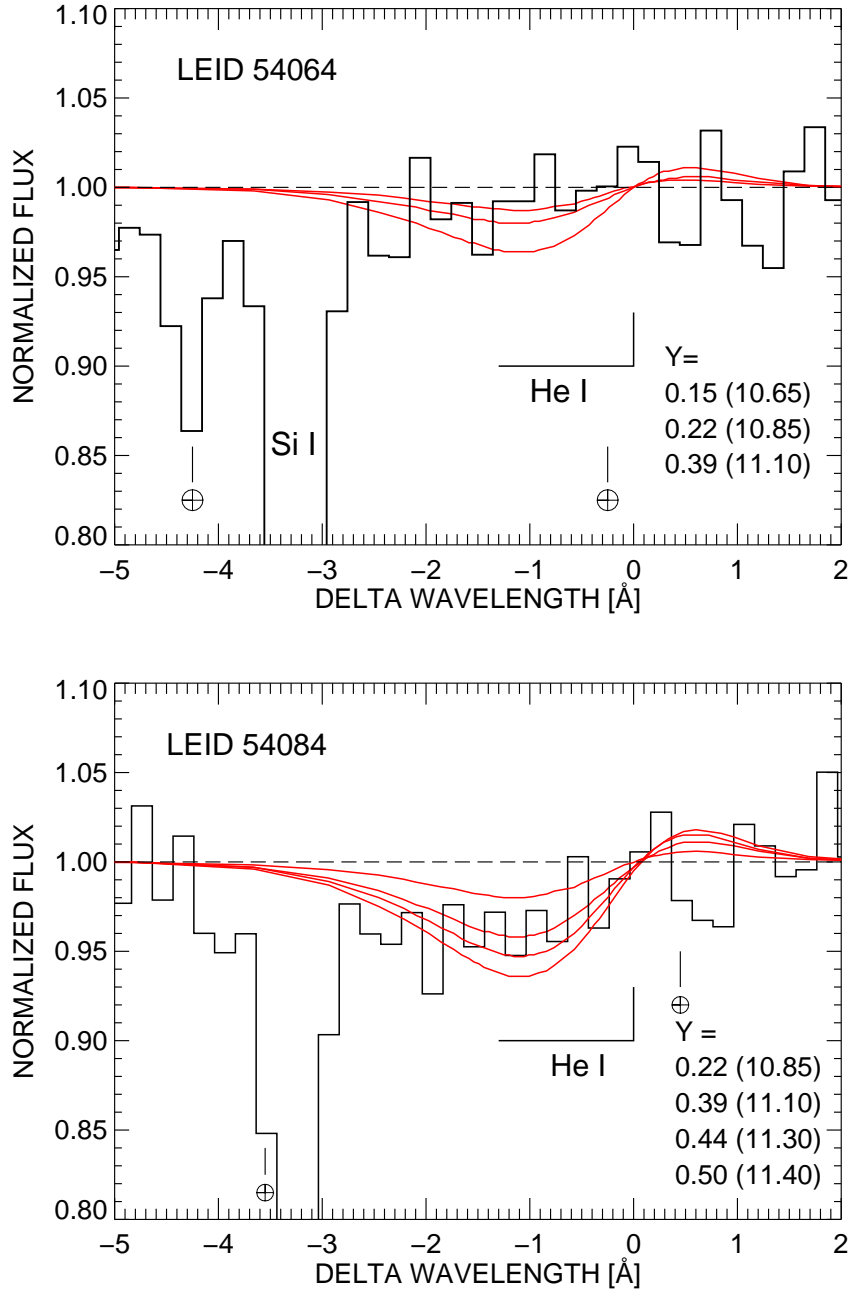


Fig. 3.— Observed Helium lines binned to a resolution element in the two matched red giants with the 10830Å profile as calculated for several values of the helium abundance (*shown by a solid smoothly varying line that is colored red in the electronic edition*). Values of  $Y$  are given for the calculated curves arranged top to bottom and the corresponding  $\log(n_{He}/n_H)$  is shown in parentheses where  $\log n_H=12.00$ .

Table 1. Characteristics of Target Stars

Quantity	LEID 54064	LEID 54084	Refs.
V	13.27	13.21	1
B–V	1.048	1.044	1
$K_s$	10.62	10.56	2
$T_{eff}$ [K]	4741	4745	3
$\log g$ [ $\text{cm s}^{-2}$ ]	1.76	1.74	3
$M_V$	–0.43	–0.49	4
$\log L/L_\odot$	2.21	2.23	5
$[Fe/H]$	–1.86	–1.79	3
$[Na/Fe]$	–0.14	0.37	3
$[Al/Fe]$	$\leq 0.36$	1.12	3
EW (He I) [ $\text{m}\text{\AA}$ ]	$\leq 9.2$	89.5	3

References. — (1) van Leeuwen et al. 2000 ;(2) 2MASS All Sky Survey; Skrutskie et al. 2006; (3) Dupree et al. 2011; (4) Distance modulus from Johnson & Pilchowski 2010; (5) Bolometric correction from Alonso et al. 1999.